High-frequency two-photon ionization of helium and cesium

M. Marinescu, H. R. Sadeghpour, and A. Dalgarno

Harvard-Smithsonian Center for Astrophysics, 60 Garden Street, Cambridge, Massachusetts 02138

Received October 13, 1992; revised manuscript received January 12, 1993

Calculations of the two-photon ionization of metastable levels of helium and the first three s levels of cesium are presented. The calculations are carried out to second order in a perturbation expansion and are valid for low laser intensities. The behavior of the ionization cross section at high photon frequencies ω is studied, and it is found that the N-photon ionization cross section behaves as $\sigma^{(N)} \propto \omega^{-(2N+1/2)}$. This analytic asymptotic behavior is verified numerically in the case of two-photon ionization.

1. INTRODUCTION

The theory of multiphoton absorption of atoms and molecules is a rapidly growing area of research activity. The introduction of stable high-powered lasers to atomic and molecular spectroscopy in the past two decades and the observation of novel phenomena such as the above-threshold structures associated with ionization and dissociation have stimulated a substantial theoretical effort, much of it using perturbation expansions of the multiphoton transition matrix elements.[1-6]

Infinite sums in the Nth order of photons involving products of N dipole matrix elements have been evaluated by several methods. Although truncation of the infinite sums has yielded reasonably accurate results near resonance lines, where a small number of discrete terms are important, it gives incorrect nonresonant values for the multiphoton matrix elements, primarily because of its neglect of the intermediate continuum. Alternatively, the infinite summation can be cast in the form of $N - 1$ inhomogeneous differential equations,[3-5] each successive equation being driven by the response function of the previous inhomogeneous equation. This method for the evaluation of perturbation transition matrix elements has been quite successful in prediction and interpretation of low laser intensity data. Some researchers have also carried out the infinite sums variationally on an L^2 discretized basis.[2,3,6]

Some nonperturbative *ab initio* methods have been proposed.[7-12] Numerical time-dependent techniques[7-9] on single-electron and multielectron atoms allow for the explicit introduction of time-dependent laser field amplitudes (pulse shape). Floquet-type expansions of the time-dependent state function[10-12] (based on the periodic nature of the light–atom interaction potential) have been developed into reliable nonperturbative methods for the study of high-order ionization and harmonic generation by medium-intensity lasers. In most of these calculations, the atom–laser interaction is treated semiclassically.

In this paper we report a calculation of two-photon excitation and ionization cross-sections of the Rydberg helium and cesium metastable levels within the framework of second-order perturbation theory.[13] Similar calculations were performed on these atoms.[14-18] Our intent is to investigate the form of the ionization cross-sections at high photon frequencies, to present highly accurate numerical results for the two-photon ionization of the atoms, and to clarify some ambiguities that exist in the literature regarding the choice of boundary conditions on the Green's function. In Section 2 the problem is discussed and a simple analytic representation of the variation of the ionization cross-section with energy is derived. In Section 3 the numerical technique is presented, and in Section 4 the results are given. Comparisons are made with experimental and other theoretical results. The asymptotic behavior of the ionization cross section at high photon frequencies is verified by comparison with numerical calculations. For the photoabsorption of cesium we discuss the implications of core polarization by the valence electron and show the modified results. In Section 5 we discuss our results.

2. THEORY

A. Two-Photon Cross Section

If we denote the initial energy of the atom as E_0, the expression for the differential two-photon ionization cross section is[19]

$$\frac{d\sigma^{(2)}}{d\Omega} = 2\pi(2\pi\alpha\omega)^2|\mathcal{M}^{(2)}|^2\frac{k_2}{(2\pi)^3}, \tag{1}$$

where the final energy of the photoelectron is $E_2 = E_0 + 2\omega$, $k_2 = (2E_2)^{1/2}$, and $\mathcal{M}^{(2)}$ is the amplitude for a two-photon transition in the second order of time-dependent perturbation theory:

$$\mathcal{M}^{(2)} = \langle f|\hat{\epsilon}\cdot\mathbf{r}G^{(+)}(E_1)\hat{\epsilon}\cdot\mathbf{r}|i\rangle. \tag{2}$$

In Eq. (2), $\langle\mathbf{r}\,|\,i\rangle = R_{nl}(r)Y_{lm}(\hat{r})$ is the wave function for the initial state and

$$\langle\mathbf{r}\,|\,f\rangle = \left(\frac{8\pi^3}{k_2}\right)^{1/2}\sum_{l'} i^{l'}\exp(-i\eta_{l'})R_{E_2l'}(r)\sum_m Y_{l'm}{}^*(\hat{k}_2)Y_{l'm}(\hat{r}) \tag{3}$$

is the outgoing wave function for the final state, where $R_{E_2l'}$ is the energy-normalized continuum radial wave function, $G^{(+)}(E_1)$ is the outgoing Green's function for the one-photon intermediate energy $E_1 = E_0 + \omega$, and $\hat{\epsilon}$ is the light polarization vector.

0740-3224/93/060988-05$06.00

The angular part of the matrix element can be worked out analytically, resulting in

$$\mathcal{M}^{(2)} = \left(\frac{8\pi^3}{k_2}\right)^{1/2} \sum_{q,q'=\pm 1} (-)^{1+(q+q')/2} \times \left[\frac{\left(l+\frac{1+q}{2}\right)\left(l+q+\frac{1+q'}{2}\right)}{(2l+1)(2(l+q)+1)}\right]^{1/2} \times (-i)^{l+q+q'} \exp(i\eta_{l+q+q'}) \times \mathbf{M}^{(+)E_2, l+q+q'}_{l+q,nl}(E_1) \sum_{ij} \epsilon_i \epsilon_j \mathcal{T}^{l+q+q', l+q}_{ij,lm}(\hat{r}), \quad (4)$$

where $\mathcal{T}^{l''l'}_{ij,lm}(\hat{r})$ are the components of an angular tensor that may be written as

$$\mathcal{T}^{l''l'}_{ij,lm} = \sum_{m'\beta} \langle l'm'1\beta \,|\, lm\rangle \mathbf{e}_i \cdot \mathbf{V}_{l''l'm'} \mathbf{e}_j \cdot \mathbf{e}_\beta, \quad (5)$$

where $\mathbf{V}_{l''l'm'}$ are the vector spherical harmonics and $\mathbf{e}_\beta$ with a Greek index β is a spherical vector.[20] $\mathbf{M}^{(+)}$ has the form

$$\mathbf{M}^{(+)E,l''}_{l',nl}(\Omega) = \int_0^\infty r^3 dr R_{El''}(r) \mathcal{A}^{(+)}_{l',nl}(\Omega; r), \quad (6)$$

in which $\mathcal{A}^{(+)}$ is the radial linear response function in the length gauge,[21]

$$\mathcal{A}^{(+)}_{l',nl}(\Omega; r) = \frac{1}{r} \int_0^\infty g^{(+)}_{l'}(\Omega; r, r') R_{nl}(r') r'^2 dr', \quad (7)$$

where $g^{(+)}_l$ is the radial outgoing Green's function with orbital quantum number l, defined such that the full Green's function is given by the partial wave expansion

$$G^{(+)}(\Omega; r, r') = \sum_l g^{(+)}_l(\Omega; r, r') \sum_m Y_{lm}(\hat{r}) Y_{lm}{}^*(\hat{r}'). \quad (8)$$

Using the well-known identity[22]

$$G^{(+)}(\Omega) = \lim_{\eta \to +0} \frac{1}{\Omega - H + i\eta} = \mathcal{P}\left(\frac{1}{\Omega - H}\right) - i\pi\delta(\Omega - H) = G^{(\mathrm{st})}(\Omega) - i\pi\delta(\Omega - H), \quad (9)$$

we can extract the imaginary part of the Green's function. The standing Green's function $G^{(\mathrm{st})}$ is a real quantity. Thus the radial linear response function can be decomposed into a real and an imaginary part as follows:

$$\mathcal{A}^{(+)}_{l',nl}(\Omega; r) = \begin{cases} \mathcal{A}^{(\mathrm{st})}_{l',nl}(\Omega; r) - i\pi R^{\Omega l'}_{nl} R_{\Omega l'}(r) & \text{if } \Omega \text{ is an eigenvalue} \\ \mathcal{A}^{(\mathrm{st})}_{l',nl}(\Omega; r) & \text{otherwise} \end{cases}, \quad (10)$$

where $\mathcal{A}^{(\mathrm{st})}$, the standing radial linear response function, has the same form as $\mathcal{A}^{(+)}$ in Eq. (7) with the radial outgoing Green's function replaced with the standing radial Green's function. In Eq. (10), $R^{El'}_{nl}$ is defined as

$$R^{El'}_{nl} \equiv \int_0^\infty R_{El'}(r) R_{nl}(r) r^3 dr. \quad (11)$$

Because $\mathcal{A}^{(\mathrm{st})}$ is a real quantity, it can be computed by the use of the Dalgarno–Lewis prescription.[23] Then $\mathcal{A}^{(\mathrm{st})}$ is the solution of the inhomogeneous differential equation

$$\left\{-\frac{1}{2}\left[\frac{1}{r^2}\frac{d}{dr}\left(r^2\frac{d}{dr}\right) - \frac{l'(l'+1)}{r^2}\right] + V(r) - E_1\right\} \mathcal{A}^{(\mathrm{st})}_{l',nl}(E_1, r) = rR_{nl}(r). \quad (12)$$

The boundary conditions on the solutions of Eq. (12) can be extracted from the integral expression for $\mathcal{A}^{(\mathrm{st})}$ in Eq. (7). In the small-r region, $\mathcal{A}^{(\mathrm{st})} \to$ constant. The application of the asymptotic boundary condition requires a more careful analysis. In fact, the large-r boundary condition is energy dependent, and we must divide the energy range into a region below the ionization threshold (case a), and a region above the ionization threshold (case b).[3,24]

In case a, $E_1 < 0$ and the first photon is absorbed below the ionization threshold. The asymptotic boundary condition corresponds to an exponential decay:

$$\mathcal{A}^{(\mathrm{st})}_{l',nl}(E_1; r) \sim 0 \quad \text{as} \quad r \to \infty. \quad (13)$$

In case b, $E_1 > 0$ and only one photon is necessary to achieve above-threshold ionization, and we have the asymptotic boundary condition

$$\mathcal{A}^{(\mathrm{st})}_{l',nl}(E_1; r) \sim -\left(\frac{2\pi}{k_1}\right)^{1/2} R^{E_1 l'}_{nl} \frac{1}{r} \cos(k_1 r - \frac{\pi}{2} l' + \delta_{l'} + \eta_{l'}) \quad \text{as} \quad r \to \infty, \quad (14)$$

where $k_1 = (2E_1)^{1/2}$, δ_l is the long-range phase shift, which for a pure Coulomb field is $\delta_l = (1/k_1)\ln 2k_1 r + \arg \Gamma[l - 1 - (i/k_1)]$, and η_l is the additional phase shift necessary to represent the short-range interaction that is due to the presence of a structured core. The phase shift η_l is zero for hydrogen but not for other atoms.

Equations (6) and (7) can now be integrated in reverse order to produce the transition matrix element $\mathbf{M}^{(+)}(E_1)$. Once this integration is accomplished, $\mathcal{M}^{(2)}$ can be calculated to give the following expression for the ionization of an s state by linearly polarized light:

$$\sigma^{(2)} = 2\pi(2\pi\alpha\omega)^2[(1/9)|\mathbf{M}^{(+)E_2 0}_{l,n0}(E_1)|^2 + (4/45)|\mathbf{M}^{(+)E_2 2}_{l,n0}(E_1)|^2], \quad (15)$$

where n is the principal quantum number for the initial state. The matrix element $\mathbf{M}^{(+)}$ in the case of above-threshold ionization always contains a real part and an imaginary part.

B. Asymptotic Energy Dependence of Cross Section

In this section we determine the order of the first term in the inverse power expansion of the photoionization cross section in ω. The cross section is given by

$$\sigma^{(2)} \propto \omega^2 |\langle f | \hat{\epsilon} \cdot \mathbf{r} G^{(+)}(E_1) \hat{\epsilon} \cdot \mathbf{r} | i \rangle|^2 k_2. \quad (16)$$

Both the Green's function and the outgoing final state can be expanded in a Born series[25] as follows:

$$G^{(+)}(\Omega) = \overline{G}^{(+)}(\Omega) \left\{\sum_{p=0}^\infty [V\overline{G}^{(+)}(\Omega)]^p\right\}, \quad (17)$$

$$\langle f | = \langle \mathbf{k}_2 | \left\{\sum_{p=0}^\infty [\overline{G}^{(+)}(\Omega) V]^p\right\}, \quad (18)$$

where $\overline{G}^{(+)}(\Omega)$ is the free-electron outgoing Green's function (see below). In this expansion, we need to concern

ourselves only with the first term in each of Eqs. (17) and (18) because we wish to obtain the leading term of the cross section at high frequencies.

Noting that

$$\langle \mathbf{r} \,|\, \mathbf{k}_2 \rangle = \exp(-i\mathbf{k}_2 \cdot \mathbf{r}) = 4\pi \sum_l i^l j_l(k_2 r) \sum_m Y_{lm}^*(\hat{k}_2) Y_{lm}(\hat{r}), \tag{19}$$

$$\bar{g}_l^{(+)}(\Omega; r, r') = 2k j_l(kr_<) h_l^{(+)}(kr_>), \tag{20}$$

where $k = (2\Omega)^{1/2}$ and j_l and $h_l^{(+)}$ are, respectively, the spherical Bessel function and the spherical Hankel function of the first kind, we can proceed to obtain the asymptotic energy dependence of the ionization matrix elements.

In the above expressions, only the conjugate product kr or kr' appears. Therefore, we make the following substitution:

$$\bar{g}_l^{(+)}(\Omega; r, r') \equiv k f_l(kr, kr'), \tag{21}$$

where f_l is a function of the products kr and kr'.

If we now introduce this expression into relation (16), we find that the radial matrix element is proportional to

$$\mathbf{M}_{l',nl}^{(+)E_2 l''}(E_1) \propto k_1 \int_0^\infty dr r^3 j_l(k_2 r) \int_0^\infty dr' r'^3 f_l(k_1 r, k_1 r') R_{nl}(r'). \tag{22}$$

In these integrals we make the substitutions $\rho = k_1 r$, $\rho' = k_1 r'$, and $\zeta = k_0/k_1 [k_0 = (2E_0)^{1/2}]$. Then

$$\mathbf{M}_{l',nl}^{(+)E_2 l''}(E_1) \propto \frac{1}{k_1^7} \int_0^\infty d\rho \rho^3 j_{l''}[(2+\zeta)\rho] \int_0^\infty d\rho' \rho'^3 f_{l'}(\rho, \rho') R_{nl}(\zeta\rho'). \tag{23}$$

For high frequencies where $\zeta \to 0$, the integrals become independent of energy, and

$$\mathbf{M}_{l',nl}^{(+)E_2 l''}(E_1) \propto 1/k_1^7 \sim \omega^{-7/2} \tag{24}$$

or $|\mathcal{M}^{(2)}|^2 \propto \omega^{-7}$, which implies that the two-photon cross sections approach zero as

$$\sigma^{(2)} \propto k_2 \omega^2 |\mathcal{M}^{(2)}|^2 \sim \omega^{-9/2}. \tag{25}$$

By repeating the argument to higher orders, we can generalize this relation of the N-photon ionization cross section to

$$\sigma^{(N)} \propto \omega^{-(2N+1/2)} \tag{26}$$

for $N > 1$.

3. NUMERICAL PROCEDURE

We have developed an efficient method for solving a set of inhomogeneous equations with particular application to multiphoton processes of atomic and molecular systems where a central field potential is present. We use the Numerov method to solve Eq. (12) subject to the boundary conditions discussed above. The differential equations are integrated from the origin on a logarithmic r scale. (A typical initial value of $x = \ln r$ for starting the integration is $x \simeq -30$.) The integration is then switched to linear r scale at $x \simeq 1.5$. The advantage of this method is that the numerical solution $\mathcal{A}(E_1; r)$ becomes insensitive to the choice of the amplitude of the wave function near the origin, which ordinarily causes difficulties in obtaining inhomogeneous solutions. Both discrete and continuum wave functions are calculated in a similar fashion near the origin and are different only in the choice of the asymptotic boundary conditions. A more detailed account of the numerical procedures will be furnished elsewhere.

Once $\mathcal{A}(E_1; r)$ has been evaluated from Eq. (12), the matrix elements in Eq. (6) are calculated with relative ease for case a, in which $\mathcal{A}(E_1; r)$ is a bound wave function. The situation is dramatically different for case b, where $\mathcal{A}(E_1; r)$ is an oscillatory wave function containing real and imaginary parts. The continuum–continuum matrix elements between $\mathcal{A}(E_1; r)$ and the final state scattering wave function of energy $E_2 = E_1 + \omega$ are computed following the procedure of Gao and Starace[26] by integrating out to the asymptotic distance $r = r_0$, beyond which WKB-type phase-amplitude wave functions are valid. The solutions are analytically continued in the complex plane, $r \to r_0 + re^{i\theta}$. Then a rotation of $\theta = \pi/2$ to the imaginary axis is performed in the upper half-plane. This rotation forces the oscillatory part of the integrand for $r \geq r_0$ to damp out exponentially, producing rapid convergence of the numerical integration.

4. RESULTS AND DISCUSSIONS

A. Helium

We show in Fig. 1 the two-photon spectra of He(2^1S) and He(2^3S) as functions of frequency. For the metastable levels of helium, we use the central field potential of Aymar and Crance,[27] who evaluated the two-photon absorption of metastable helium below the single ionization threshold. Above the ionization threshold at $\omega = 32\,014.11$ cm^{-1}, both the real and the imaginary parts in expression (14) contribute. Below the threshold, the spectra are identical to the results of Aymar and Crance.[27]

B. Cesium

To represent the cesium valence electronic states, we use the parametric model potential of Greene.[28] This l-dependent model potential includes the effect of the Cs^+ core polarization that is due to the electric field of the valence electron.

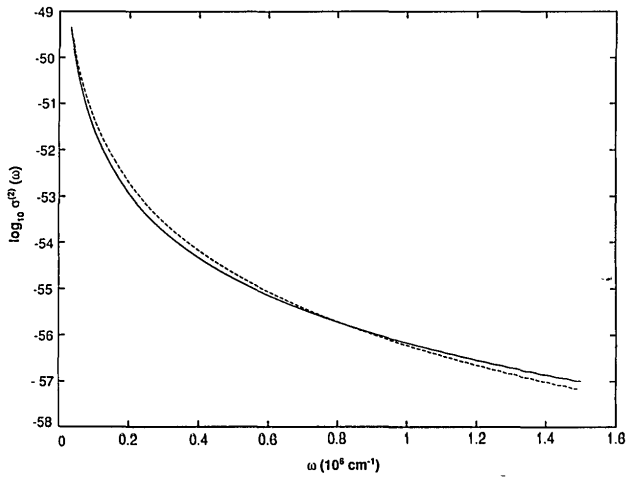

Fig. 1. Above-threshold ionization cross sections of He(2^1S) (solid curve) and He(2^3S) (dashed curve) metastable states as functions of the incident photon frequency.

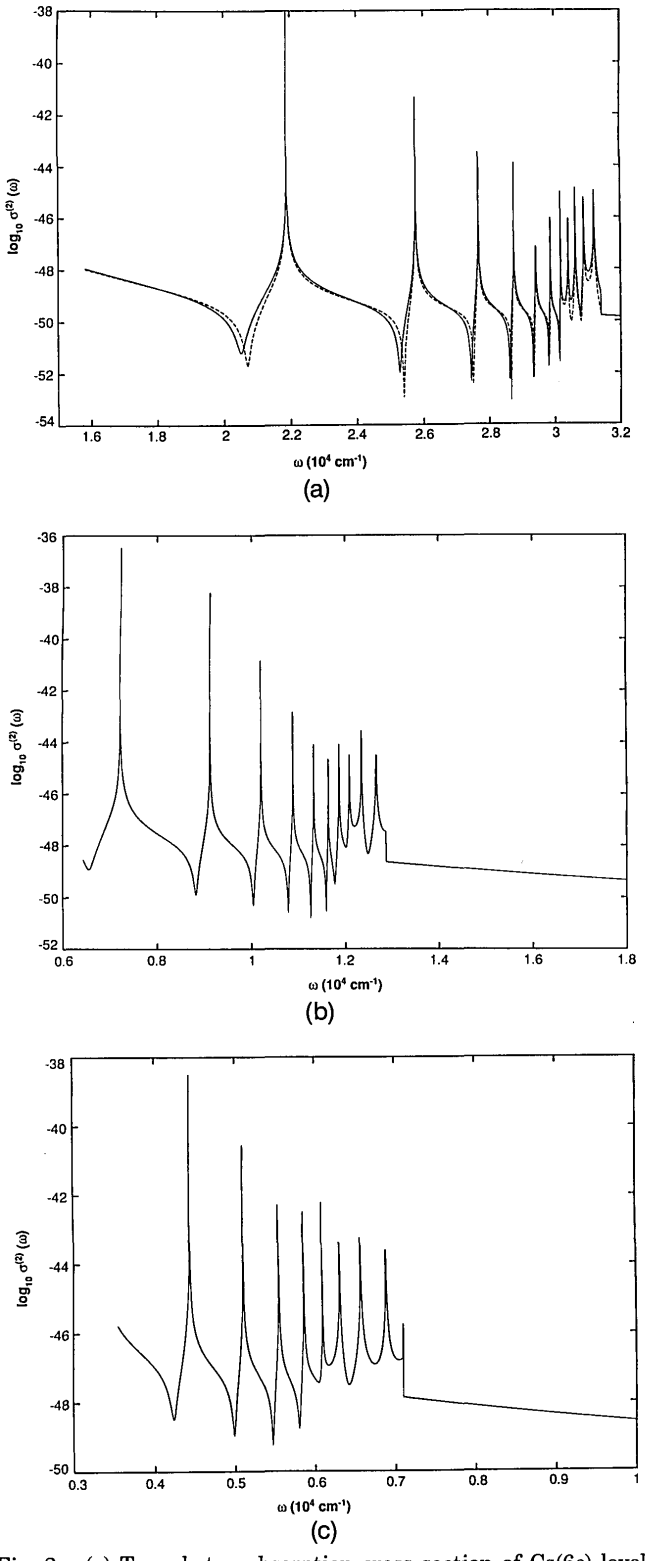

Fig. 2. (a) Two-photon absorption cross section of Cs(6*s*) level. The dashed curves refer to the modified form of the cross section when we use the dressed dipole operator. The first peak is due to the Cs(6*p*) level. (b) Same as in (a) for Cs(7*s*) level. (c) Same as in (a) for Cs(8*s*) level.

Figures 2(a), 2(b), and 2(c) give the two-photon absorption cross sections of the Cs(6*s*), Cs(7*s*), and Cs(8*s*) states, respectively, as functions of ω. The precursors to the intermediate *np* Rydberg resonances in these spectra are the 6*p*, 7*p*, and 8*p* Rydberg resonances. In Fig. 3 we display the ionization cross sections of the cesium levels up to 9 a.u. above the 6*s* ionization threshold. The simple power-law dependence of the cross section with photon energy confirms the predicted $\omega^{-9/2}$ variations. In Fig. 4 the fictitious cross sections from the real and the imaginary components of the matrix element in Eq. (6) are shown for the ionization of the cesium ground state together with the total cross section. The Cooper minimum of 67 500 cm^{-1} (to be compared with the value of 67 728.4 cm^{-1} from Seaton[29]) is evident in the imaginary part of the matrix element, which effectively gives the one-photon ionization cross section, aside from the multiplicative dipole coupling of the intermediate continuum state to the final state. The imaginary component produces a substantial contribution to the total cross section. Indeed, at a frequency of 743 000 cm^{-1}, the imaginary part of the matrix element overtakes the real part and becomes the dominant contribution to the total ionization cross section.

In the model potential method for cesium, the effect of the external electric field of the valence electron on the

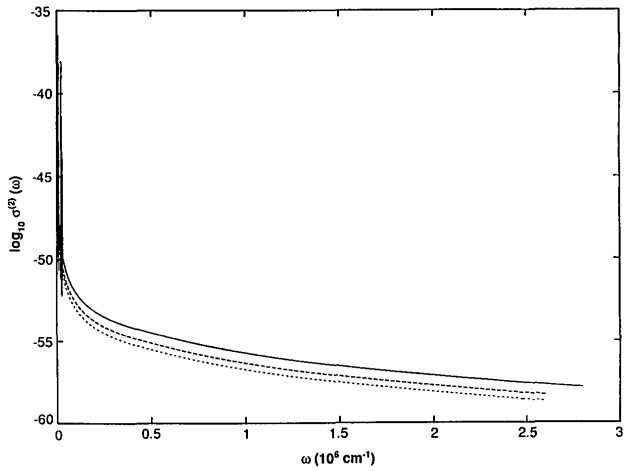

Fig. 3. Above-threshold ionization of Cs(6*s*) (solid curve), Cs(7*s*) (dashed curve), and Cs(8*s*) (dotted curve) levels. Note the simple power-law dependence of the cross section as $\omega^{-9/2}$ with photon frequency.

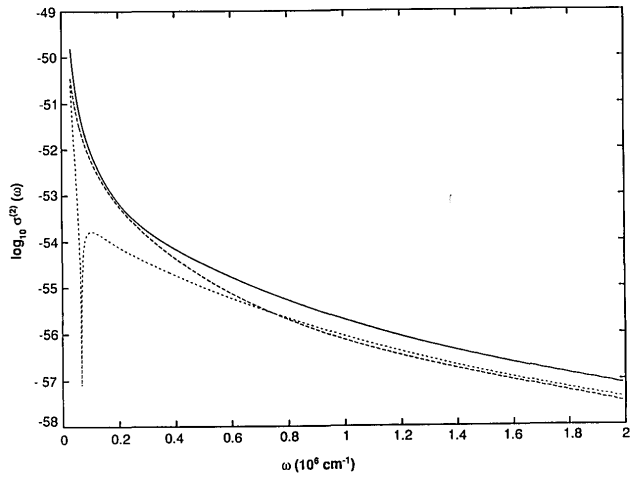

Fig. 4. The real (dashed curve) and imaginary (dotted curve) fictitious two-photon cross sections from Eq. (6) for the ionization of the cesium ground state. The Cooper minimum at 67 500 cm^{-1} appears in the imaginary cross section. Also note that the two components cross at $\omega \sim 7 \times 10^5$ cm^{-1}. The total cross section is shown as the solid curve.

closed-shell core Cs^+ is incorporated by adding a polarization term to the dipole operator.[30,31] This electric-field perturbation, whose value at the nucleus is $-\mathbf{r}/r^3$, where $\mathbf{r}$ is the electric dipole moment of the valence electron, induces a dipole moment in the core, whose value is now proportional to $-\mathbf{r}/r^3$ such that the total dipole moment is $\mathbf{r}(1 - \alpha_c/2r^3)$. Accordingly, we replace the dipole operator as

$$\mathbf{r} \ll \mathbf{r}\left(1 - \frac{\alpha_c}{2r^3}\{1 - \exp[-(r/r_c)^3]\}\right), \tag{27}$$

where α_c, the polarizability of Cs^+, and r_c, the cutoff radius, are the parameters of the model potential. Sadeghpour and Dalgarno[32] showed that the inclusion of this dressed dipole corrects for the discrepancy between the experimental and uncorrected model values of the cesium static polarizability.

A typical spectrum of cesium two-photon ionization with the dressed dipole is given in Fig. 2(a) as dashed curves. The discrepancy between the calculated curves with bare and dressed dipole operators is greatest near absorption lines. Because the adiabatic following of the core polarization with the electric field of the valence electron and the eventual repulsion of the core from the outer electron tends to reduce the discrete oscillator strengths, we expect a general lowering of the absorption profile strengths for the low-lying p levels.

5. SUMMARY

We present results for two-photon excitation and ionization of helium and cesium in the lowest-order perturbation expansion. The infinite sums over the intermediate discrete and continuum states are handled by the inhomogeneous differential equation method. Boundary conditions on the inhomogeneous solutions are treated so as to allow for the absorption of a single photon in the continuum.

The calculations take into account the virtual free–free absorption of a photon for He $l = 0$ metastable states and for $l = 0$ ground and metastable states of cesium. We find that the high-frequency limit of the $\sigma^{(2)}$ ionization cross section behaves as $\omega^{-9/2}$, a finding supported by numerical calculations. The states of helium and cesium are described by parametric model potentials of Aymar and Crance and by Greene, respectively. The cesium potential includes a term that accounts for the polarization of Cs^+ core of the electric field of the valence electron. The effect of this polarization on the electric dipole moment is investigated, and we find that the effect is largest near bound absorption lines, implying that the bound oscillator strength distribution of cesium is appreciably modified by the inclusion of the core polarization in the electric dipole moment.

ACKNOWLEDGMENTS

H. R. Sadeghpour and A. Dalgarno were supported by the U.S. Department of Energy, Division of Chemical Sciences, Office of Basic Energy Sciences, Office of Energy Research. M. Marinescu was supported by the Smithsonian Predoctoral Fellowship Program.

REFERENCES

1. B. A. Zon, N. L. Manakov, and L. P. Rapaport, Sov. Phys. JETP **34,** 515 (1972).
2. Bo Gao and A. F. Starace, Phys. Rev. Lett. **61,** 404 (1988); Phys. Rev. A **39,** 4550 (1989).
3. M. Edwards, X. Tang, P. Lambropoulos, and R. Shakeshaft, Phys. Rev. A **33,** 4444 (1986); M. Edwards, X. Tang, and R. Shakeshaft, Phys. Rev. A **35,** 3758 (1987).
4. M. Aymar and M. Crance, J. Phys. B **14,** 3585 (1981); **15,** 719 (1982).
5. F. Robicheaux and Bo Gao, Phys. Rev. Lett. **67,** 3066 (1991).
6. E. Karule, Adv. Atom. Mol. Opt. **27,** 256 (1991).
7. K. C. Kulander, Phys. Rev. A **38,** 778 (1988).
8. J. M. Javanainen and J. H. Eberly, J. Phys. B **21,** L93 (1988).
9. M. S. Pindzola and C. Bottcher, J. Opt. Soc. Am. B **4,** 752 (1987).
10. M. Horbatsch, J. Phys. B **24,** 4919 (1991).
11. R. M. Potvliege and R. Shakeshaft, Phys. Rev. A **40,** 3061 (1989).
12. M. Pont, Phys. Rev. A **44,** 2141 (1991).
13. A. Dalgarno, in *Perturbation Theory and its Applications in Quantum Mechanics,* C. H. Wilcox, ed. (Wiley, New York, 1966), pp. 145–183.
14. W. Zernik and R. W. Klopfenstein, J. Math. Phys. **6,** 262 (1965).
15. C. Klarsfeld, Lett. Novo Cimento **3,** 395 (1970).
16. M. R. Teague and P. Lambropoulos, Phys. Rev. A **14,** 1067 (1976).
17. A. Kassaee, M. L. Rustgi, and S. A. T. Long, Phys. Rev. A **37,** 999 (1988).
18. H. Bachau, P. Lambropoulos, and X. Tang, Phys. Rev. A **42,** 5801 (1990).
19. F. H. M. Faisal, *Theory of Multiphoton Processes* (Plenum, New York, 1987).
20. V. Florescu, A. Halasz, and M. Marinescu, Phys. Rev. A **47,** 394 (1993).
21. V. Florescu and T. Marian, Phys. Rev. A **34,** 4641 (1986).
22. H. A. Bethe and E. E. Salpeter, *Quantum Mechanics of One- and Two-Electron Atoms* (Springer-Verlag, Berlin, 1955).
23. A. Dalgarno and J. T. Lewis, Proc. R. Soc. London Ser. A **259,** 424 (1960).
24. M. Aymar and M. Crance, J. Phys. B **14,** 3585 (1981).
25. A. Messiah, *Quantum Mechanics* (North-Holland, Amsterdam, 1961).
26. B. Gao and A. F. Starace, Computers Phys. **1**(6), (1987).
27. M. Aymar and M. Crance, J. Phys. B **13,** 2527 (1980).
28. C. H. Greene, Phys. Rev. A **42,** 1405 (1990).
29. M. J. Seaton, Proc. R. Soc. London Ser. A **208,** 418 (1951).
30. S. Hameed, A. Herzenberg, and M. G. James, J. Phys. B **1,** 822 (1968).
31. H. L. Zhou and D. W. Norcross, Phys. Rev. A **40,** 5048 (1989).
32. H. R. Sadeghpour and A. Dalgarno, J. Phys. B **25,** 4801 (1992).